Distribution of AVP and Ca2+-dependent PKC-isozymes in the suprachiasmatic nucleus of the mouse and rabbit

van der Zee, Eddy A.; Bult, Abel

Published in:
Brain Research

DOI:
10.1016/0006-8993(95)00968-1

Publication date:
1995

ELSEVIER

Brain Research 701 (1995) 99–107

BRAIN RESEARCH

Research report

Distribution of AVP and Ca^{2+}-dependent PKC-isozymes in the suprachiasmatic nucleus of the mouse and rabbit

Eddy A. Van der Zee [a,*], Abel Bult [b]

[a] *Department of Cell and Molecular Biology, Northwestern University Medical School, 303 East Chicago Avenue, Chicago, IL 60611–3008, USA*
[b] *Child Study Center, Yale University School of Medicine, PO Box 207900, New Haven, CT 06520–7900, USA*

Accepted 11 July 1995

Abstract

The suprachiasmatic nucleus (SCN) is the circadian pacemaker in mammals and contains a network of arginine-vasopressin-immunoreactive (AVP-ir) neurons. AVP-recipient cells contain the V1a class of receptors linked to phosphoinositol turnover and protein kinase C (PKC). The present study describes the localization of AVP and the four Ca^{2+}-dependent PKC-isoforms in the mouse and rabbit SCN. An estimate of the numerical density of AVP-ir neurons at the rostral, medial, and caudal level of the SCN revealed that the mouse SCN contains more than twice the number of AVP-ir neurons than the rabbit SCN. Neurons immunostained for AVP or PKC dominated in the dorsomedial and ventrolateral aspects of the mouse SCN, while the central area of the SCN revealed only weakly stained neurons. The rabbit SCN was characterized by a more homogeneous distribution of AVP-ir and PKC-ir neurons. PKCα was the most abundantly expressed isozyme in both species, whereas the presence of the other isoforms differed (mouse: PKCα > PKCβI > > PKCβII > PKCγ; rabbit: PKCα > PKCβII ≥ PKCγ > PKCβI). Clear PKCγ-positive neurons were only observed in the rabbit SCN, while the mouse SCN predominantly contained immunolabeled fiber tracts for this PKC isozyme. Astrocytes immunoreactive for each PKC isoform were frequently encountered in the rabbit SCN, but were absent in mice. Immunofluorescence double labeling showed that numerous AVP-recipient cells in the mouse SCN were immunopositive for PKCα, and that nearly all AVP-ir neurons express PKCα abundantly. These results substantiate the putative role for PKCα in vasopressinergic signal transduction in the SCN. The differential expression in degree and cell type of the Ca^{2+}-dependent PKC-isoforms in the mouse and rabbit SCN may be related to the differences observed in circadian timekeeping between the two species.

Keywords: Astrocyte; Calcium; Immunocytochemistry; Protein kinase C; Suprachiasmatic nucleus; Vasopressin

1. Introduction

The mammalian suprachiasmatic nucleus (SCN), the circadian pacemaker [16,23,27,35], contains a local arginine-vasopressin (AVP) circuit. AVP-immunoreactive (AVP-ir) neurons form soma-somatic appositions and have extensive synaptic relationships with other AVP-positive and AVP-negative neurons in both the ipsi- and contralateral SCN [5,48]. In addition, AVP-positive fibers arising from the SCN project to other hypothalamic regions [6,11]. AVP-ir neurons in the mouse SCN have been implicated in relaying timing information of circadian wheel-running activity [3], and these neurons represent a neuronal substrate which functionally correlates with the expression of circadian rhythmicity in common voles [8]. AVP-induced responses of SCN cells in slices of the hamster hypothalamus and mediated by V1a receptors [20]. V1a receptors and transcripts have been demonstrated in the SCN by receptor autoradiography and in situ hybridization, respectively [18,32,33,46,53]. Stimulation of V1a receptors results in phosphoinositol turnover and the subsequent activation of protein kinase C (PKC) [38,43]. Nadakavukaren and coworkers [29] demonstrated the presence of the phosphoinositol transduction system in the SCN of rats, indicating that PKC is present in the SCN. PKC is a key protein involved in signal transduction and a variety of physiological processes [30]. Four different Ca^{2+}-dependent PKC-isoforms have been identified, and differences in regional and subcellular distribution suggest diverse physiological functions for the different isoforms [30,45,47]. AVP exerts an excitatory effect on SCN neurons in vitro [20,24,25,39], suggesting that the activation of

* Corresponding author. Fax: (1) (312) 503–7912. E-mail: eavdzee@merle.acns.nwu

SSDI 0006-8993(95)00968-X

PKC contributes to the circadian cycle of electrical activity in the SCN. The distribution and functional role of the different PKC isozymes in the SCN, however, is currently unknown.

The aim of the present study was to describe the localization of the Ca^{2+}-dependent PKC-isoforms in the mouse and rabbit SCN employing antibodies raised against the α, βI, βII, and γ isoforms. The choice of mice and rabbits was based on the differences in entrainment to the LD-cycle and the number of AVP-ir neurons in the SCN between the two species. Whereas mice are exclusively nocturnal, rabbits are only predominantly nocturnal under undisturbed conditions [12–15], and AVP-ir cells in the mouse SCN seem to outnumber those in the rabbit SCN [4,37].

2. Materials and methods

Adult male mice (*Mus domesticus*, 3–4 months of age, $n = 10$) and young adult female New Zealand albino rabbits (*Oryctolagus cuniculus*, 3 months of age, $n = 6$) were used for this study. The animals were individually housed under a 12:12 LD cyclus with food and water available ad libitum. The animals were deeply anesthetized and transcardially perfused during the first half of the light period with 3–4% paraformaldehyde, 0.05% glutaraldehyde and 0.2% picric acid in 0.1 M phosphate buffer (PB) (pH 7.4), which was preceded by a short prerinse of saline. The brains were removed from the skull and cryoprotected by overnight storage at 4°C in 30% sucrose in 0.1 M PB. Subsequently, the brains were coronally sectioned on a cryostat microtome at a thickness of 20 μm.

PKC isoforms were visualized by means of polyclonal rabbit IgG antibodies raised against the catalytic subdomain of the α, βI, βII, and γ isoforms (C-20, C-16, C-18 and C-19, respectively; Santa Cruz Biotechnology, Inc.). AVP was visualized employing the polyclonal IgG antibody rabbit anti-AVP (Truus; an antibody graciously supplied by Dr. R.M. Buijs of the Netherlands Institute for Brain Research). Free floating brain sections were preincubated with 5% normal goat serum (NGS) in phosphate-buffered saline (PBS) for 30 min, and thereafter incubated overnight under gentle movement with the primary antibody solution in (PBS) containing a PKC isoform selective rabbit-anti PKC IgG (1:100) or Truus (1:1000). Triton X-100 (0.5%) was added during all incubation steps in the AVP-staining procedure. After rinsing in PBS and a preincubation in NGS for 30 min, the sections were exposed for 2 h at room temperature (RT) to biotinylated goat anti-rabbit IgG (F(ab')2 fraction, 1:200; Amersham). Subsequently, the sections were thoroughly rinsed in PBS and incubated with Steptavidin-HRP (2 h at RT, 1:200; Amersham). The sections were again rinsed in PBS and Tris buffer, and reacted under visual guidance with diaminobenzidine (DAB) (30 mg DAB in 100 ml Tris buffer, pH 7.4) and 0.01% H_2O_2. Finally, the sections were mounted and coverslipped for light microscopic inspection.

Cell counts for AVP-ir neurons in the rabbit SCN were performed in 6 sections per animal containing the rostral ($n = 2$), medial ($n = 2$), and caudal ($n = 2$) level. The SCN levels in these sections of the rabbit SCN match levels of the mouse SCN as described before (respectively level 2, 8 and 14, see Fig. 3, Bult et al., 1992 [4]), and the surface area (mm^2) of the SCN is comparable. Neurons were only counted when the nucleus was in the plane of section. All AVP-ir neurons in the SCN in the chosen sections were counted (left + right side). The numbers were averaged per level per animal, and finally the numbers of all animals were averaged per level and presented in Fig. 2.

Immunofluorescence double-labeling was carried out for PKCα and AVP to demonstrate the expression of PKCα in AVP-positive and AVP-recipient neurons. For this purpose we used the mouse monoclonal M4 raised against the catalytic subdomain of PKCα (1:400; a generous gift of Dr. K.L. Leach). The incubation in the primary antibodies was performed simultaneously overnight, like described above, in the presence of 0.1% Triton X-100 during all incubation steps. Brain sections were subsequently incubated in a mixture of Phycoerythrin-conjugated goat anti-rabbit IgG (Tago, 1:200) and biotinylated rabbit anti-mouse-IgM (1:50) for 2 h at RT. After rinsing in PBS the sections were exposed to fluorescein isothiocyanate (FITC)-conjugated Streptavidin (Zymed, 1:50, 2 h at RT). Thereafter, the sections were mounted and coverslipped in a 1:1 mixture of PBS and glycerin. The sections were studied and photographed with a Ploemopak Leitz fluorescent microscope with the appropriate filter blocks for FITC and Phycoerythrin labels, yielding a green and red fluorescence, respectively.

3. Results

3.1. AVP-immunoreactivity in mouse and rabbit SCN

AVP-immunoreactivity in the mouse and rabbit SCN differed primarily in the intranuclear distribution and numerical density of labeled neurons and terminals (Fig. 1). The mouse SCN was characterized by two clusters of AVP-ir neurons; a large one in the dorsomedial area and a smaller one in the ventrolateral area (Fig. 1A). The central area of the SCN contained few AVP-positive neurons (arrows in Fig. 1A). However, numerous AVP-ir terminals were found throughout the mouse SCN, and a dense plexus of immunopositive fibers was seen in the dorsal portion. The rabbit SCN contained fewer AVP-ir neurons (Fig. 1B) and terminals, scattered more homogenously throughout the region without forming distinct intranuclear clusters. Immunopositive fibers were only rarely encountered. The

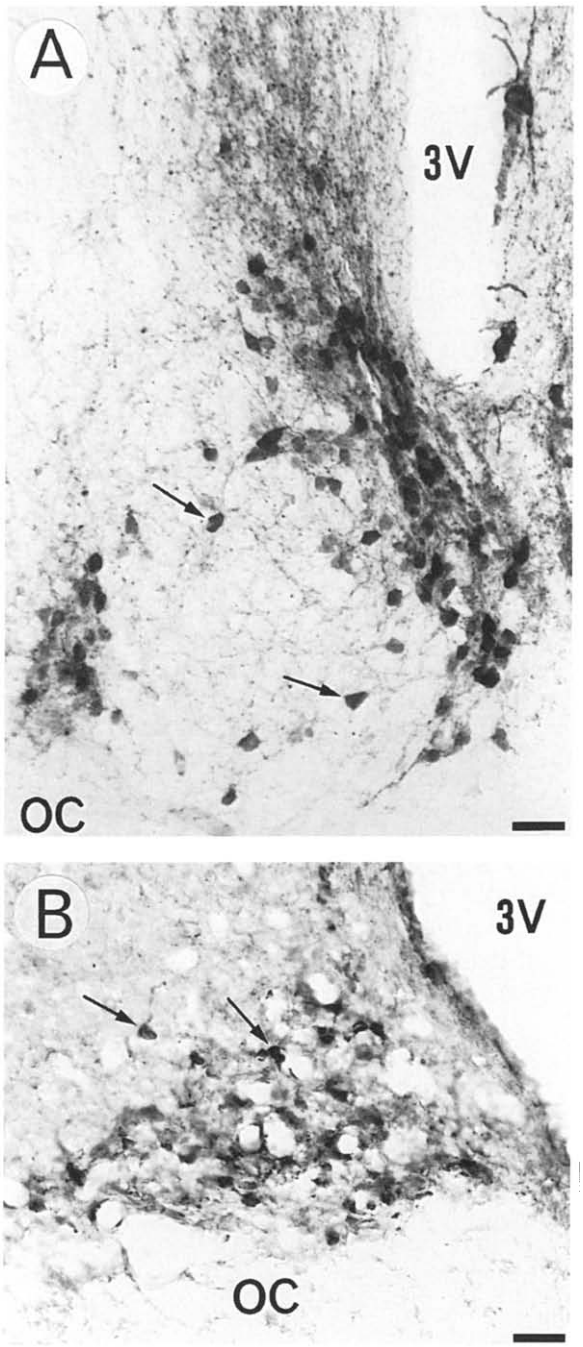

Fig. 1. AVP-immunoreactivity at the middle level of the mouse (A) and rabbit (B) SCN. At this coronal level, AVP-immunoreactivity in the mouse SCN is characterized by densely packed neurons in the dorsomedial and ventrolateral subdivisions, whereas the neurons in the rabbit SCN are scattered throughout the region. The general shape and size of the neurons (arrows), however, are similar for mice and rabbits. Numerous and relatively few AVP-positive fibers and terminals are seen in the mouse and rabbit SCN, respectively. 3V = third ventricle; OC = Optic Chiasm; Scale bar = 22 μm.

vast majority of rabbit AVP-ir neurons was lightly stained, whereas in the mouse the majority of the AVP-ir neurons was densely stained. In contrast, the staining intensity of AVP-ir neurons of the paraventricular nucleus, present in the same immunostained sections, was more similar in both species. Cell counts in six brain sections of each animal containing the rostral, middle, and caudal level of the left and right SCN revealed a 1.9, 2.4 and 2.8 fold higher number of AVP-ir neurons in mice than in rabbits, respectively (Fig. 2). Combining all levels, the mouse SCN contains approximately 2.3 times the number of AVP-ir neurons. These cell counts further show that although the numerical density and local distribution of AVP-ir neurons differs in both species, the overall pattern in the rostrocaudal axis is fairly similar (Fig. 2).

3.2. PKC-isoform immunoreactivity in mouse and rabbit SCN

The mouse SCN is clearly delineated by PKCα and βI-immunoreactivity. The immunoprecipitates were primarily associated to the neuronal cell membrane, and the nuclei of the SCN neurons were immunonegative for any PKC isoform. No PKC-ir astrocytes were found in the SCN. Semi-quantification of the staining intensity of the immunopositive neurons is presented in Table 1, showing that the level of immunoreactivity ranks: PKCα > PKCβI > > PKCβII > PKCγ. PKCα was most abundantly expressed in the mouse SCN. Numerous, tightly packed immunopositive cells were found throughout the SCN, although the neurons in the dorsomedial and ventrolateral subdivisions were stained more intensely than in the central subdivision (Fig. 3A). The neurons were round to slightly elongated in shape, and ranged from 8–10 μm in diameter. Well stained dendrites were less frequently encountered. Some immunopositive axons were found in the optic chiasm (OC). Moderate staining for PKCβI was

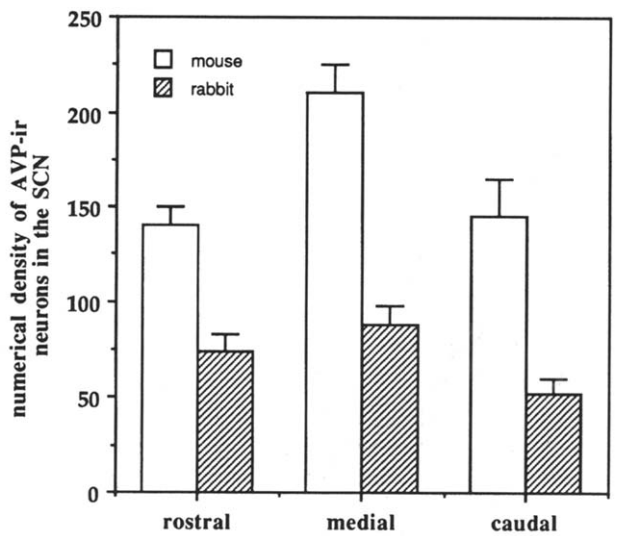

Fig. 2. Cell counts of the AVP-ir neurons in mouse (obtained from Bult et al., 1992 [4]) and rabbit at a comparable rostral, medial, and caudal level of the SCN. The numerical density of AVP-ir neurons in the mouse SCN is respectively 1.9, 2.4, and 2.8 fold higher at these levels than in the rabbit SCN.

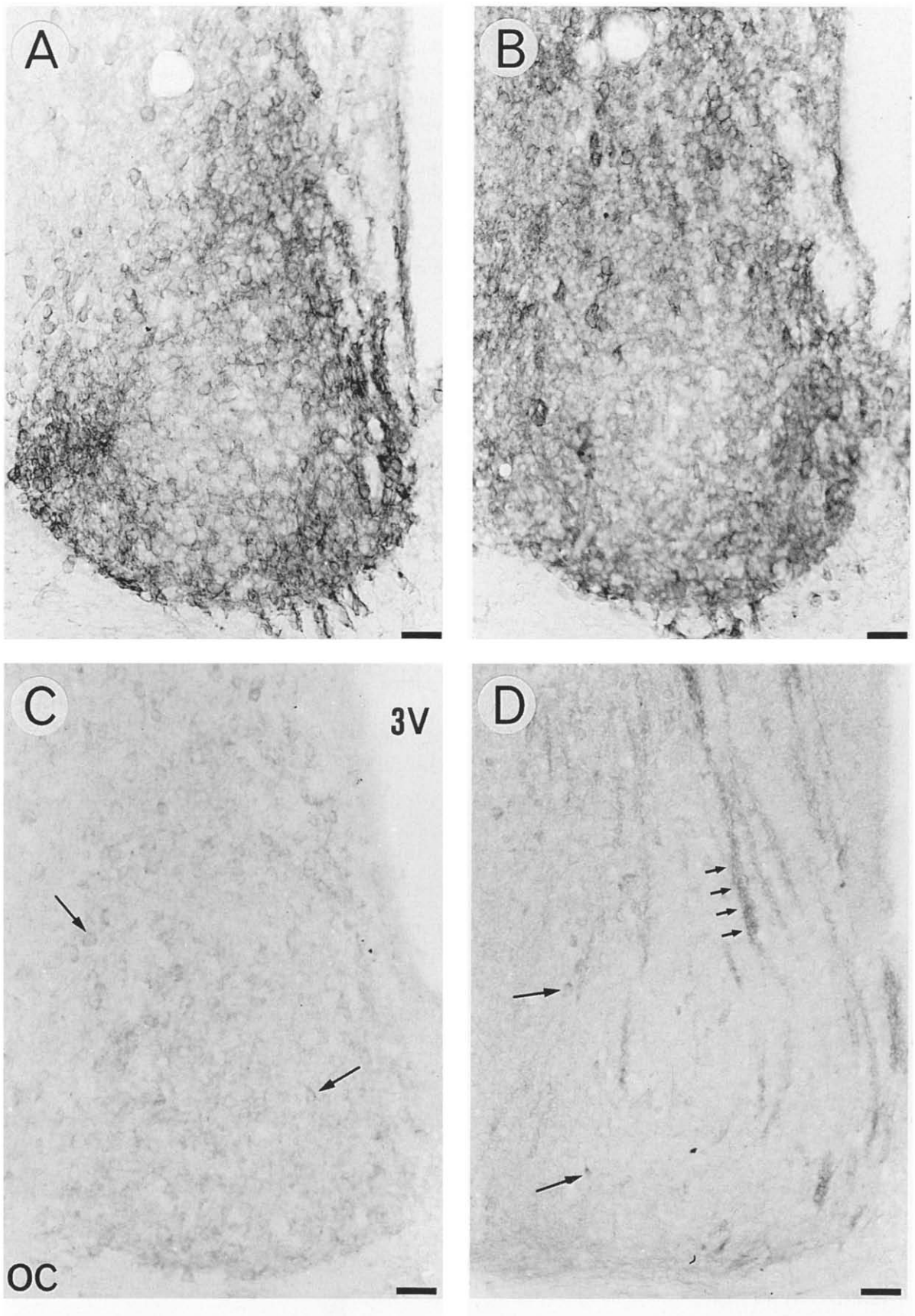
A
B
C
3V
OC
D

Table 1
Staining intensity of neurons for the different PKC isozymes in the SCN of mouse and rabbit

	Mouse	Rabbit
PKCα	+ + + +	+ + +
PKCβI	+ + +	+
PKCβII	+	+ +
PKCγ	−	+ +

Semi-quantification of the staining intensity. −: absent; +: weak; + +: moderate; + + +: dense; + + + +: very dense.

found in tightly packed neurons in all SCN subdivisions (Fig. 3B). The distribution and size of these neurons resembled those immunoreactive for PKCα. Labeled fibers were frequently encountered in the OC. In contrast to PKCα and PKCβI, only few clearly stained neurons were found for PKCβII, whereas a large number of neurons revealed very weak levels of labeling (Fig. 3C). No stained elements were found in the OC for PKCβII. PKCγ-ir was only present in some fiber bundles, and rarely an immunopositive neuron could be found in the SCN (Fig. 3D).

The PKC-immunoreactivity in the rabbit SCN only partially resembled the mouse SCN (Table 1). Compared to the mouse, the rabbit SCN was relatively small and, except for PKCα, less clearly delineated by PKC-immunoreactivity. The rabbit SCN was typically characterized by astrocytes stained for all PKC subspecies. These astrocytes were scattered throughout the SCN region, but PKCα-positive astrocytes tended to be more clustered in the vicinity of small blood vessels (Fig. 5A). Processes of notably PKCγ-positive astrocytes were wrapped around the larger blood vessels in the SCN (Fig. 5B). Semi-quan-

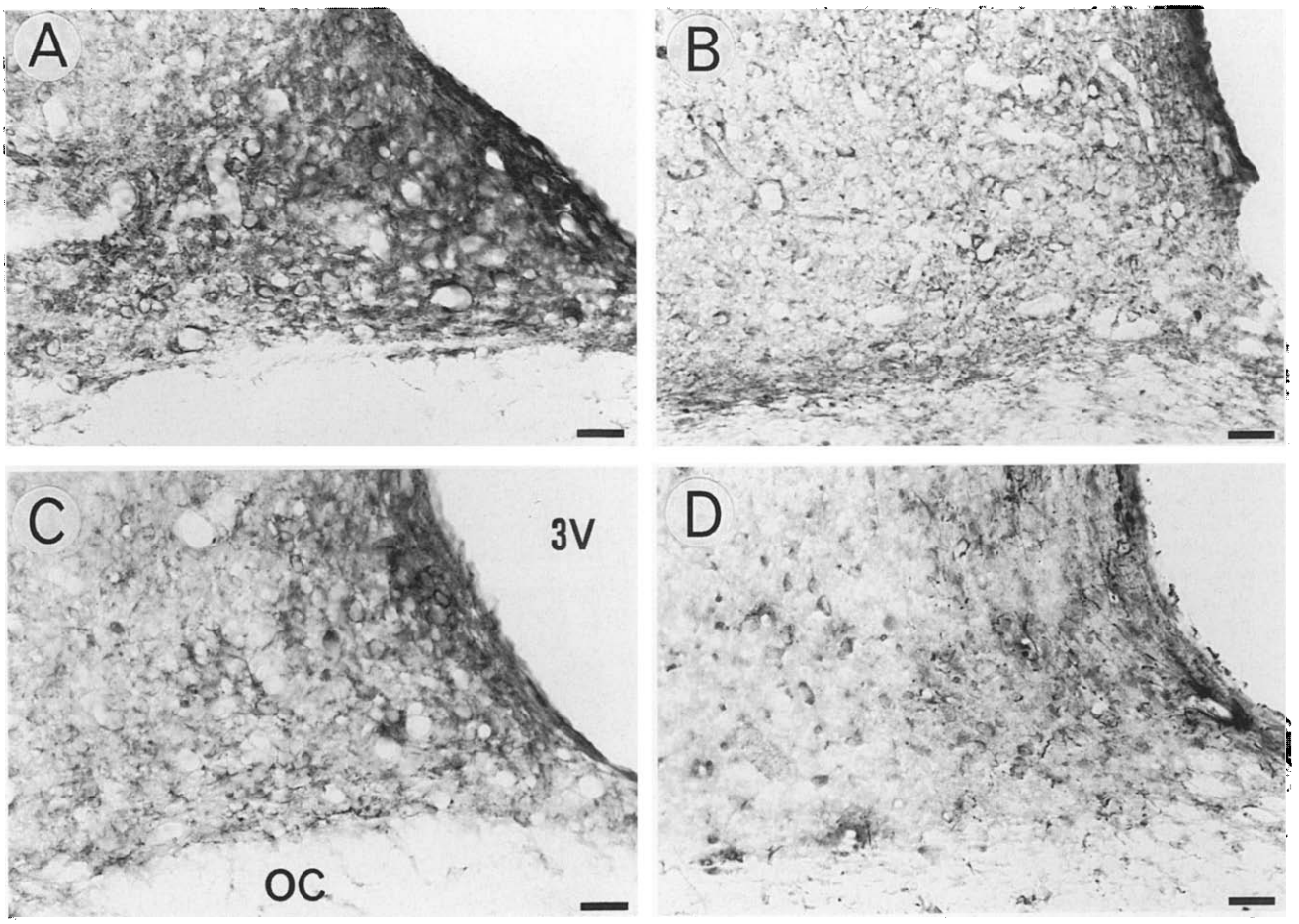

Fig. 4. Distribution of the Ca^{2+}-dependent PKC-isoforms in the rabbit SCN. PKCα (A) is most abundantly expressed in the SCN neurons, followed by PKCβII (C), PKCγ (D) and PKCβI (B). The rabbit SCN is characterized by a relatively homogeneous distribution of PKC-ir neurons. PKC-positive astrocytes were frequently observed in the SCN and OC, most notably for PKCα and γ. 3V = third ventricle; OC = Optic Chiasm; Scale bar = 22 μm.

Fig. 3. Distribution of the Ca^{2+}-dependent PKC-isoforms in the mouse SCN. PKCα (A) and PKCβI (B) are most abundantly expressed, whereas PKCβII (C) and PKCγ (D) are weakly expressed. Neurons immunoreactive for PKCα and βI are densely packed, notably at the rim of the SCN while the central portion contains weaker stained neurons. PKCβII is somewhat more homogeneously expressed, although at a low level (arrows in C). PKCγ is almost absent in the SCN, and could only be encountered in few cells and fiber tracts (large and small arrows in D, respectively). 3V = third ventricle; OC = Optic Chiasm; Scale bar = 22 μm.

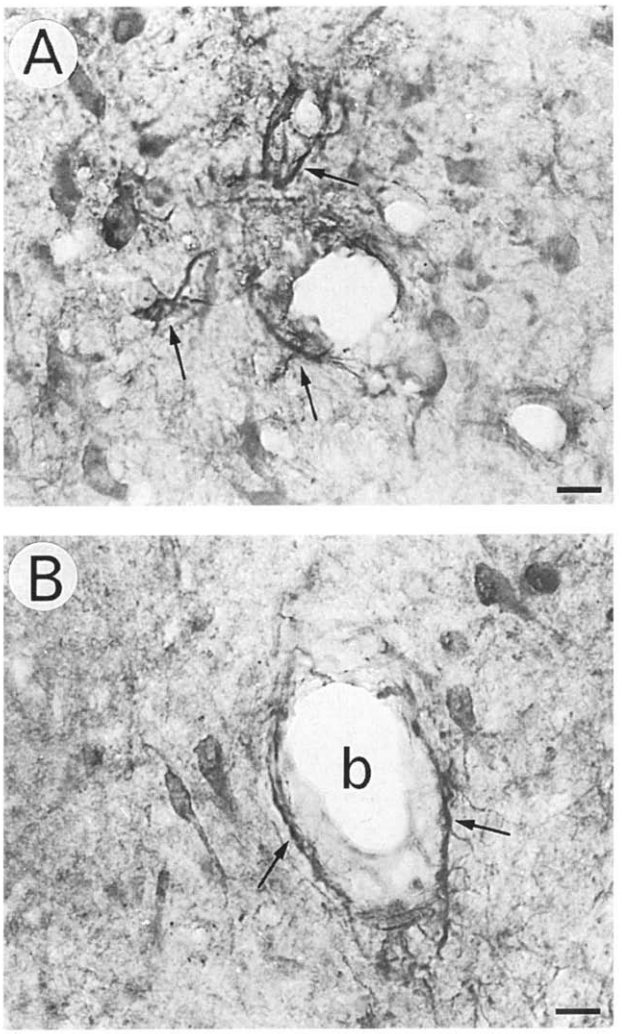

Fig. 5. PKC isozyme immunoreactivity in astrocytes in the rabbit SCN. PKCα, βI, βII, and γ-positive astrocytes are found scattered throughout the SCN. Notably PKCα-positive astrocytes (arrows in A) tend to be clustered in the vicinity of small blood vessels. Processes of PKCγ-positive astrocytes (arrows in B) were frequently found wrapped around the larger blood vessels. b = blood vessel; Scale bar = 10 μm.

tification of the staining intensity of the immunoreactive neurons is presented in Table 1, showing that PKCα > PKCβII $\geq$ PKCγ > PKCβI. Like in the mouse, PKC-immunoreactivity was predominantly associated to the cell membrane, and the nuclei of the neurons were devoid of PKC-immunoreactivity. PKCα was found in many neurons and in the neuropil (Fig. 4A). These cells were predominantly small (10–12.5 μm) and round with few immunoreactive dendrites. Densely stained astrocytes were found in the OC. Few scattered, round to elongated shaped neurons expressed PKCβI (Fig. 4B). Some immunoreactive astrocytes and fibers were encountered in the OC. The neuropil was relatively faintly stained. Numerous tightly packed neurons were found for PKCβII of similar size and shape as the neurons immunoreactive for the α isoform (Fig. 4C). Small astrocytes and some fibers were present in the OC. PKCγ-immunoreactivity revealed moderately to densely stained neurons of 10–15 μm, often of an elongated cell type scattered throughout the SCN (Fig. 4D), and several immunoreactive astrocytes, both in the SCN and OC. PKCγ-immunoreactivity in the SCN neurons was more diffuse than that of the other isoforms.

3.3. Colocalization of AVP and PKCα in mouse SCN

The distribution of PKCα in the mouse and rabbit SCN studied with the monoclonal antibody M4 appeared to be similar to that obtained with the polyclonal antibody C-20 (data not shown). The PKCα-positive neurons largely outnumbered the AVP-positive neurons. Immunofluorescence double-labeling revealed that nearly all AVP-ir neurons of the mouse SCN express PKCα (Fig. 6). No difference was observed between the two clusters of AVP neurons in the dorsomedial and ventrolateral divisions. The

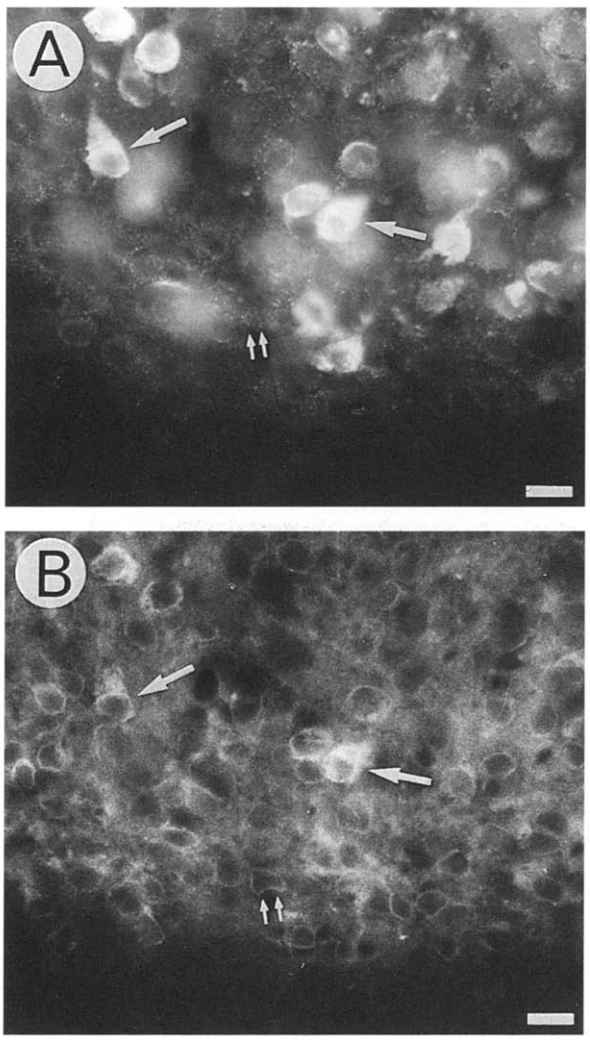

Fig. 6. Immunofluorescence double-labeling for AVP (A) and PKCα (B) in the mouse at the border of the dorsal SCN and the optic chiasm. The vast majority of AVP-ir neurons express PKCα (large arrows). Numerous PKCα-positive SCN neurons are contacted by delicate AVP-positive terminals (small arrows). Scale bar = 10 μm.

AVP-ir neurons generally contained the highest concentration of PKCα (large arrows in Fig. 6). The immunolabeling for the α isoform was predominantly restricted to the cell membrane region of the neuron, whereas AVP was more diffusely distributed in the cytoplasm. AVP-ir terminals were frequently found around PKCα-ir neurons, which were either AVP-positive or AVP-negative (small arrows in Fig. 6).

4. Discussion

4.1. Specificity of polyclonal antibodies

Weak cross-reactivity to certain other protein kinase C isoforms has recently been reported (Santa Cruz Biotechnology, Inc.) for the polyclonal antibodies C-20, C-16, and C-18 raised against PKCα, -βI, and -βII, respectively. No cross-reactivity was found with the polyclonal antibody C-19 raised against PKCγ. C-20 cross-reacts weakly with PKCβ. No such cross-reactivity has been reported for the anti-PKCα monoclonal M4, and the distribution and staining intensity for both antibodies were very similar in the mouse and rabbit SCN. This suggests that the cross-reactivity of C-20 in this study can be neglected. Due to the weak cross-reactivity of C-16 and C-18, however, we cannot exclude that a minor part of the obtained immunocytochemical distribution for PKCβI and PKCβII reflects other PKC isoforms.

4.2. Distribution of AVP and PKC isoforms in SCN

The mouse and rabbit SCN contain high numbers of AVP-ir neurons and terminals impinging upon numerous SCN cells. The number and distribution of AVP-ir neurons varies between mammals [42], and the numerical density differs more than two-fold between rabbits and mice (this study). The AVP-recipient cells are known to contain V1a-receptors linked to phosphoinositol turnover and subsequent PKC activation. Indeed, the SCN of both species contains numerous PKC-positive neurons, with a distribution resembling the location of AVP-ir terminals. Immunofluorescent double-labeling revealed that neurons surrounded by AVP-ir terminals express PKCα. Therefore, we conclude that the majority of the PKCα-expressing SCN neurons are AVP-recipient cells, including the AVP-ir neurons themselves. The AVP-ir neurons generally express the highest levels of PKCα. These findings suggest that PKCα plays a key role in vasopressinergic neurotransmission, and further demonstrates the interconnected character of the AVP-ir neuronal circuitry in the SCN as previously demonstrated at the electron microscopic level [5,48].

To our knowledge this study is the first report describing the distribution of the four Ca^{2+}-dependent PKC-isozymes in the mammalian SCN. The results show that the distribution and degree of PKC-immunoreactivity differs between mouse and rabbit. The most pronounced difference was found for PKCγ. SCN neurons of the mouse do not express PKCγ, which is identical to the SCN of rats (E.A. Van der Zee, unpublished observations) and chickens [50]. In contrast, neurons in the rabbit SCN do contain PKCγ, although these neurons are somewhat differentially shaped and distributed compared to the neurons expressing the α, βI, and βII isoforms. Differences in the distribution of PKC isoforms across animals species have been reported frequently, and may reflect species-specific roles for the PKC isozymes [1,45,47].

In the OC of mouse and notably rabbit, numerous PKC-ir fibers were seen. Axons of the optic tract and associated astrocytes are known to contain PKC isoforms [17]. Part of the neuropil staining in the SCN, therefore, may represent PKC-ir terminals arising from the optic nerves.

4.3. Functional role of PKC isoforms in SCN

The physiological function of PKC in the SCN is currently unknown. PKC plays a critical role in regulating neuronal signal transduction, and the expression of PKC in AVP-recipient cells substantiate their role in vasopressinergic signal transduction in the SCN. Besides AVP, however, several other neurotransmitter systems in the SCN may activate PKC through their receptors, for example the excitatory amino acids of the visual input or the cholinergic input from the forebrain and brain-stem [2,28]. PKC may therefore mediate intracellular cross talk between AVP and other neurotransmitter systems. Lithium, acting directly on the SCN [19], is known to decrease phosphoinositol turnover [9,34], and subsequently decreases the function of PKC. Lithium lengthens the free-running circadian period in many species [10,19], and suppresses neuronal firing of SCN neurons [22]. Lithium also decreases membrane-associated PKCα, without affecting either the β or γ isoforms [21]. PKCα is the most abundantly expressed isoform in the mouse and rabbit SCN, and the effect of lithium suggests a role for PKCα in clock function.

A remarkable species difference became apparent in the PKC expression of astrocytes. The rabbit SCN contains astrocytes immunoreactive for all Ca^{2+}-dependent PKC-isoforms, whereas the astrocytes in the mouse SCN are PKC-immunonegative. Besides SCN neurons [40,41,44], also astrocytes show an intracellular Ca^{2+} increase in response to neurotransmitter stimulation, suggesting a role of astrocytes in clock function of the SCN [49]. Calcium waves through astroglial gapjunctions may be important for circadian rhythm generation, and the integration of astrocytes may lend greater stability to the circadian oscillator [49]. However, PKC activation in astrocytes blocks gapjunction communication and inhibits the spread of calcium waves [7]. High levels of PKC expression in astrocytes of the SCN may therefore reduce clock function. It is

tempting, therefore, to speculate that abundant expression of PKC in astrocytes of the rabbit SCN correlates with the weaker circadian rhythmicity in rabbits compared to mice [12,15]. Circadian timing is known to be disturbed in aging and age-related changes in glia are observed in the SCN [26,31,36]. Previously, Van der Zee and coworkers [51] described a significant increase in number and staining intensity of glial cells expressing abundant numbers of cholinergic receptors in the aging rat SCN, which represent reactive astrocytes [52]. In conclusion, these observations suggest that a high level of expression of proteins involved in signal transduction in astrocytes of the SCN may result in reduced clock function and weakening of the circadian pacemaker.

Acknowledgements

Part of this work was supported by the Netherlands Organization for Scientific Research (NWO) to E.A. Van der Zee.

References

[1] Battaini, F., Lucchi, L., Bergamaschi, S., Ladisa, V., Trabucchi, M. and Govoni, S., Intracellular signaling in the aging brain – The role of protein-kinase-C and its calcium-dependent isoforms, *Ann. N.Y. Acad. Sci.*, 719 (1994) 271–284.

[2] Bina, K.G., Rusak, B. and Semba, K., Localization of cholinergic neurons in the forebrain and brain-stem that project to the suprachiasmatic nucleus of the hypothalamus in rat, *J. Comp. Neurol.*, 335 (1993) 295–307.

[3] Bult, A., Hiestand, L., Van der Zee, E.A. and Lynch, C.B., Circadian rhythms differ between selected mouse lines: a model to study the role of vasopressin neurons in the suprachiasmatic nuclei, *Brain Res. Bull.*, 32 (1993) 623–627.

[4] Bult, A., Van der Zee, E.A., Compaan, J.C. and Lynch, C.B., Differences in the number of arginine-vasopressin-immunoreactive neurons exist in the suprachiasmatic nuclei of house mice selected for differences in nest-building behavior, *Brain Res.*, 578 (1992) 335–338.

[5] Castel, M., Feinstein, N., Cohen, S. and Harari, N., Vasopressinergic innervation of the mouse suprachiasmatic nucleus: an immunoelectron microscopic analysis, *J. Comp. Neurol.*, 298 (1990) 172–187.

[6] De Vries, G.J., Buijs, R.M., van Leeuwen, F.W., Caffé, A.R. and Swaab, D.F., The vasopressinergic innervation of the brain in normal and castrated rats, *J. Comp. Neurol.*, 233 (1985) 236–254.

[7] Enkvist, M.O. and McCarthy, K.D., Activation of protein kinase C blocks astroglial gap junction communication and inhibits the spread of calcium waves, *J. Neurochem.*, 59 (1992) 519–526.

[8] Gerkema, M.P., Van der Zee, E.A. and Feitsma, L.E., Expression of circadian rhythmicity correlates with the number of arginine-vasopressin-immunoreactive cells in the suprachiasmatic nucleus of common voles, Microtus arvalis, *Brain Res.*, 639 (1994) 93–101.

[9] Hallcher, L.M. and Sherman, W.R., The effects of lithium and other agents on the activity of myo-inositol-1-phosphatase from bovine brain, *J. Biol. Chem.*, 255 (1980) 10896–10901.

[10] Hoffman, K., Günderoth-Palmowski, M., Wiedermann, G. and Engelmann, W., Further evidence for the lengthening effect of Li^+ on circadian rythms, *Z. Naturforsch.*, 33c:231–234

[11] Hoorneman, E.M. and Buijs, R.M., Vasopressin fiber pathways in the rat brain following suprachiasmatic nucleus lesioning, *Brain Res.*, 243 (1982) 235–241

[12] Jilge, B., The rabbit: a diurnal or a nocturnal animal?, *J. Exp. Animal Sci.*, 34 (1991) 170–183

[13] Jilge, B., The ontogeny of circadian rythms in the rabbit, *J. Biol. Rythms*, 8 (1993) 247–260

[14] Jilge, B. and Stahle, H., The internal synchronization of five circadian functions of the rabbit, *Chronobiol. Int.*, 1 (1984) 195–204

[15] Kennedy, G.A., Hudson, R. and Armstrong, S.M., Circadian wheel running activity rhythms in two strains of domestic rabbit, *Physiol. Behav.*, 55 (1994) 385–389

[16] Klein, D.C., Moore, R.Y. and Reppert, S.M. (Eds.), *The Mind's Clock*, Oxford University Press, New York, 1991, 467 pp.

[17] Komoly, S., Liu, Y., Webster, H.D. and Clan, K.F., Distribution of protein kinase C isozymes in rat optic nerves, *J. Neurosci. Res.*, 29 (1991) 379–389.

[18] Kremarik, P., Freund-Mercier, M.J. and Stoeckel, M.E., Oxytocin and vasopressin binding sites in the hypothalamus of the rat: histoautoradiographic detection, *Brain Res. Bull.*, 36 (1995) 195–203

[19] LeSauter, J. and Silver, R., Lithium lengthens the period of circadian rhythms in lesioned hamsters bearing SCN grafts, *Biol. Psychiatry*, 34 (1993) 75–83.

[20] Liou, S.Y. and Albers, H.E., Single unit response of suprachiasmatic neurons to arginine vasopressin (AVP) is mediated by a V_1-like receptor in the hamster, *Brain Res.*, 477 (1989) 336–343.

[21] Manji, H., Etcheberrigaray, R., Chen, G. and Olds, J.L., Lithium decreases membrane-associated protein kinase C in hippocampus: selectivity for the α isozyme, *J. Neurochem.*, 61 (1993) 2303–2310.

[22] Mason, R. and Biello, S.M., A neurophysiological study of a lithium-sensitive phosphoinositide system in the hamster suprachiasmatic (SCN) biological clock in vitro, *Neurosci. Lett.*, 144 (1992) 135–138.

[23] Meijer, J.H. and Rietveld, W.J., Neurophysiology of the suprachiasmatic circadian pacemaker in rodents, *Physiol. Rev.*, 69 (1989) 671–707.

[24] Mihai, R., Coculescu, M., Wakerly, J.B. and Ingram, C.D., The effects of [ARG^8]vasopressin and [ARG^8]vasotocin on the firing rate of suprachiasmatic neurons in vitro, *Neuroscience*, 62 (1994) 783–792

[25] Mihai, R., Juss, T.S. and Ingram, C.D., Suppression of suprachiasmastic nucleus neurone activity with a vasopressin receptor antagonist: possible role for endogenous vasopressin in circadian activity cycles in vitro, *Neurosci. Lett.*, 179 (1994) 95–99.

[26] Mirmiran, M., Swaab, D.F., Kok, J.H., Hofman, M.A., Witting, W. and Van Gool, W.A., Circadian rhythms and the suprachiasmatic nucleus in perinatal development, aging and Alzheimer's disease, *Prog. Brain Res.*, 93 (1992) 151–162.

[27] Moore, R.Y., Organization and function of a central nervous system circadian oscillator: the suprachiasmatic hypothalamic nucleus, *Fed. Proc.*, 42 (1983) 2783–2789.

[28] Morin, L.P., The circadian visual system, *Brain Res. Rev.*, 19 (1994) 102–127.

[29] Nadakavukaren, J.J., Welsh, D.K. and Reppert, S.M., Aluminium fluoride reveals a phosphoinositide system within the suprachiasmatic region of the rat hypothalamus, *Brain Res.*, 507 (1990) 181–188.

[30] Nishizuka, Y., Studies and perspectives of protein kinase C, *Science*, 233 (1986) 305–312.

[31] Ogata, R., Age-related morphological changes in the rat suprachiasmatic nucleus. Correlation with age-related changes in circadian rhythmicity of gross activity, *Fukuoka Acta Med.*, 77 (1986) 437–457.

[32] Ostrowski, N.L., Lolait, S.J. and Young III, W.S., Cellular localization of vasopressin V1a receptor messenger ribonucleic acid in adult male rat brain, pineal, and brain vasculature, *Endocrinology*, 135 (1994) 1511–1528.

[33] Phillips, P.A., Abrahams, J.M., Kelly, J., Paxinos, G., Grzonka, Z.,

Mendelsohn, F.A.O. and Johnston, C.I., Localization of vasopressin binding sites in rat brain by in vitro autoradiography using a radioiodinated V_1 receptor antagonist, *Neuroscience*, 27 (1988) 749–761.

[34] Ragan, C.I., Watling, K.J., Gee, N.S., Aspley, S., Jackson, R.G., Reid, G.G., Baker, R., Billington, D.C., Barnaby, R.J. and Leeson, P.D., The dephosphorylation of inositol 3,4 biphosphate to inositol in liver and brain involves two distinct Li-sensitive enzymes and proceeds via inositol-4-phosphate, *Biochem. J.*, 249 (1988) 143–148.

[35] Rusak, B. and Zucker, I., Neural regulation of circadian rhythms, *Physiol. Behav.*, 59 (1979) 449–526.

[36] Satinoff, E., Li, H., Tcheng, T.K., Liu, C., McArthyr, A.J., Medanic, M. and Gillette, M.U., Do the suprachiasmatic nuclei oscillate in old rats as they do in young ones?, *Am. J. Physiol.*, 265 (1993) R1216–R1222.

[37] Schimchowitsch, S., Moreau, C., Laurent, F. and Stoeckel, M.E., Distribution and morphometric characteristics of oxytocin- and vasopressin-immunoreactive neurons in the rabbit hypothalamus, *J. Comp. Neurol.*, 285 (1989) 304–324.

[38] Shewey, L.M. and Dorsa, D.M. V1-type vasopressin receptors in rat brain septum: binding characteristics and effects on inositol phospholipid metabolism, *J. Neurosci.*, 8 (1988) 1671–1677.

[39] Shibata, S. and Moore, R.Y., Neuropeptide Y and vasopressin effects on suprachiasmatic nucleus neurons in vitro, *J. Biol. Rhythms*, 3 (1988) 265–276.

[40] Shibata, S., Newman, G.C. and Moore, R.Y., Effects of calcium ions on glucose utilization in the rat suprachiasmatic nucleus in vitro, *Brain Res.*, 426 (1987) 332–338.

[41] Shibata, S., Shiratsuchi, A., Liou, S.Y. and Ueki, S., The role of calcium ions in circadian rhythm of suprachiasmatic nucleus neurons activity in rat hypothalamic slices, *Neurosci. Lett.*, 52 (1984) 181–184.

[42] Sofroniew, M.W. and Weindl, A., Identification of parvocellular vasopressin and neurophysin neurons in the suprachiasmatic nucleus of a variety of mammals including primates, *J. Comp. Neurol.*, 193 (1980) 659–675.

[43] Thibonnier, M., Signal transduction of V1-vascular vasopressin receptors, *Regul. Pept.*, 38 (1992) 1–11.

[44] Thomson, A.M., Slow, regular discharge in suprachiasmatic neurones is calcium dependent, in slices of rat brain, *Neuroscience*, 13 (1984) 761–767.

[45] Tominaga, S., Saito, N., Tsujino, T. and Tanaka, C., Immunocytochemical localization of α-, βI-, βII-, γ-subspecies of protein kinase C in the motor and premotor cortices of the rhesus monkey, *Neurosci. Res.*, 16 (1993) 275–286.

[46] Tribollet, E., Barberis, C., Jard, S., Dubois-Dauphin, M. and Dreifuss, J.J., Localization and pharmacological characteristics of high affinity binding sites for vasopressin and oxytocin in the rat brain by light microscopic autoradiography, *Brain Res.*, 442 (1988) 105–118.

[47] Tsujino, T., Kose, A., Saito, N. and Tanaka, C., Light and electron microscopic localization of βI-, βII- and γ-subspecies of protein kinase C in rat cerebral neocortex, *J. Neurosci.*, 10 (1990) 870–884.

[48] van den Pol, A.N. and Gores, T., Synaptic relationships between neurons containing vasopressin, gastrin-releasing peptide, vasoactive intestinal polypeptide, and glutamate decarboxylase immunoreactivity in the suprachiasmatic nucleus: dual ultrastructural immunocytochemistry with gold-substituted silver peroxidase, *J. Comp. Neurol.*, 252 (1986) 507–521.

[49] van den Pol, A.N., Finkbeiner, S.M. and Cornell-Bell, A.H., Calcium excitability and oscillations in suprachiasmatic nucleus neurons and glia in vitro, *J. Neurosci.*, 12 (1992) 2648–2664.

[50] Van der Zee, E.A., Bolhuis, J.J., Solomonia, R.O., Horn, G. and Luiten, P.G.M., Differential distribution of protein kinase C (PKCα,β and -γ) isoenzyme immunoreactivity in the chick brain, *Brain Res.*, 676 (1995) 41–52.

[51] Van der Zee, E.A., Streefland, C., Strosberg, A.D., Schröder, H. and Luiten, P.G.M., Colocalization of muscarinic and nicotinic receptors in cholinoceptive neurons of the suprachiasmatic region in young and aged rats, *Brain Res.*, 542 (1991) 348–352.

[52] Van der Zee, E.A., De Jong, G.I., Strosberg, A.D. and Luiten, P.G.M., Muscarinic acetylcholine receptor-expression in astrocytes in the cortex of young and aged rats, *Glia*, 8, (1993) 42–50.

[53] Young, W.S. III, Kovács, K. and Lolait, S.J., The diurnal rhythm in vasopressin V1a receptor expression in the suprachiasmatic nucleus is not dependent on vasopressin, *Endocrinology*, 133 (1993) 585–590.